Control and Cybernetics

vol. **34** (2005) No. 1

A new approach for simultaneous shape and topology optimization based on dynamic implicit surface function

by

Xu Guo[1], Kang Zhao[1] and Michael Yu Wang2

[1]State Key Laboratory of Structural Analysis for Industrial Equipment
Department of Engineering Mechanics, Dalian University of Technology
Dalian 116023, China

[2]Department of Automation & Computer-Aided Engineering
The Chinese University of Hong Kong Shatin
N.T., Hong Kong

Abstract: In the present paper, a new approach for structural topology optimization based on dynamic implicit surface function (DISF) is proposed. DISF is used to describe the shape/topology of a structure, which is approximated in terms of the nodal values. Then, a relationship is established between the element stiffness and the values of the implicit surface function on its four nodes. In this way and with some non-local treatments of the design sensitivities, not only the shape derivative but also the topological derivative of the optimal design can be incorporated in the numerical algorithm in a unified way. Numerical experiments demonstrate that by employing this approach, the computational efforts associated with DISF (and level set) based algorithms can be diminished. Clear optimal topologies and smooth structural boundaries free from any sign of numerical instability can be obtained simultaneously and efficiently.

Keywords: topology optimization, implicit surface function, topological derivative, level set.

1. Introduction

Topology optimization is one of the most challenging research topics in the field of structural optimization. It has received more and more research attention recently because of its great potential of application in many industrial areas. Since the pioneering work of Bendsøe and Kikuchi (1998), various approaches have been developed in the past decades to deal with this problem. We will not review the extensive literature here. For an up-to-date review of this area, we refer the readers to Eschenauer, Olhoff (2001) and the references therein.

The area of topology optimization of continuum structures is now dominated by methods that employ the material distribution concept. The typical ones are

the homogenization approach (Bendsøe and Kikuchi, 1998), and the variable density approach (SIMP) (Bendsøe, 1989, Rozvany, Zhou and Birker, 1992). In homogenization (or microstructure) based approach, the well-posedness of the topology optimization is achieved by introducing the porous materials with microstructure into the optimization model. The effective macroscopic properties of the porous materials are computed by applying some smear-out techniques. These effective properties are closely related to the microscopic geometry parameters, thus we can optimize the structural topology by adjusting these parameters. In variable density approach, a density function $\rho(x)$ ($0 \leq \rho(x) \leq 1$) is introduced into the problem formulation to represent the material distribution in the design domain. In order to achieve the goal of topology design, the density function $\rho(x)$ is related to the stiffness of the material by a power law. This choice has the effect of penalizing the intermediate densities (i.e. for $\rho(x)$ such that $0 < \rho(x) < 1$), since in this case volume is proportional while stiffness is less than proportional to $\rho(x)$. In this way, it is hoped that the optimal structure may almost entirely consist enrirely of elements which only have 0 or 1 densities. It is worth noting that most of the numerical algorithms based on these two approaches are element-based. In the element-based computational framework, the initial design space is always discretized by uniform rectangular finite elements and the design variables are assumed to be constant within each finite element.

Although element-based computational framework is quite efficient in computation and has been applied successfully in solving many industrial optimization problems, it still has some undesirable features. Most of them stem from the raster parameter model used in the problem formulation. By employing this model, a finite element grid is used both for representing the topology of the structure and performing physical analysis. As pointed out in Bendsøe (1999), this coupling effect may bring some difficulties when stress and vibration constraints are considered, since these constraints are very difficult to handle without a correct constraint/objective functional formulation (Cheng, Guo, 1997, Duysinx, Bendsøe, 1998, Petersen, 2000). Another disadvantage of the element-based optimization model is that in the representation of the geometric information, such as the location and shape of the boundary, the normal vector or curvature of the boundary are not straightforward. Therefore, the optimal design with topology-dependent loads, in which the direction and location of the applied loads may alter as the topology/shape of the structure changes, is very difficult to deal with in the raster-geometry based computational framework, since in this case the boundaries between solid and void are always not well-defined. Finally, it is well known that the optimal topologies obtained with the element-based algorithms always have zigzag boundaries. For practical considerations, a subsequent shape optimization process is required to alleviate the phenomenon of stress concentration. Therefore we must map the raster geometry model to a smooth surface model. Unfortunately, the mapping is not always straightforward and requires extra computational effort.

In order to overcome the above-mentioned undesirable features, some more geometry-oriented topology optimization algorithms have been proposed recently. The distinctive feature of these methods is the introduction of a function that describes the shape and topology of the structure implicitly. Since most of these methods use the zero level set of the dynamic implicit surface function (DISF, Osher, Fedkiw, 2003) to represent the boundary of the structure, they are also called the level set methods. The basic idea of the DISF based approach for the solution of the shape/topology optimization problems is to evolve the implicit surface function dynamically based on the sensitivities of the objective and constraint functionals.

Structural optimization by level set approach was initiated by Sethian and Wiegmann (2000). In their work, they tried to find a design with minimum weight while meeting a specified compliance constraint at the same time. A Hamilton-Jacobi equation has been used for tracing the motion of the structural boundary based on ad hoc constructed speed function. In Osher and Santosa (2001), the level set technique was applied to a model problem involving a vibrating system whose resonant frequency or spectral gap was to be optimized under volume constraint.

Notable features of this work are that the authors have used functional gradients to calculate the velocity field for level set evolution and projected gradient approach to deal with the volume constraint.

In Allaire, Jouve and Toader (2002, 2004), a computational framework for shape/topology optimization by level set method has been introduced. Shape gradient has been used to evolve the level set function and the numerical algorithm for the solution of level set function has also been presented. Wang et al. (2003, 2004) obtained the same results independently. In their papers, numerous numerical examples have been presented to demonstrate the performance of the level set approach, which can serve as valuable benchmarks for further research. Moverover, they also generalized the level set method to handle the optimal topology design problems with multi-materials (Wang and Wang, 2004). Within the framework of level set approach, topology design with topology-dependent load has been addressed by Guo, Zhao and Gu (2004). Implicit surface function has also been employed by Ruiter and Keulen (2003, 2004) for the solution of topology design problems. In their approach, exponential bias functions had been used to generate the DISF. Genetic and optimality criteria methods were used to find the optimal values of the coefficients of the bias functions.

Recently, Belytschko, Xiao and Parimi (2003) proposed an alternative approach for topology optimization of continuum structures with topology-independent loads. In their work, nodal values of the implicit function that describes the topology/shape of the structure have been used as design variables directly. A fixed-point type optimality criteria approach had been employed to find the optimal solution. Numerical examples were also presented for demonstration of the effectiveness of the approach.

Compared with traditional element-based topology optimization method, node-based optimization approach has the obvious advantage that it can describe the geometry of the structure in a more straightforward way. In every step of optimization, all the geometric information is embedded in the surface function implicitly. This is a very attractive feature when shape/topology dependent loads or boundary conditions are taken into consideration. Furthermore, apart from the flexibility of dealing with the change of the structural topology naturally, it is also very convenient for subsequent shape optimal design by this approach, since no mapping or projection is required to link the two processes.

Although DISF based approach has good potential for the solution of the problems that are difficult to deal with in the traditional element-based optimization framework, it still has some limitations.

The first one is associated with the DISF based approaches which employ the Hamilton-Jacobi equation and conventional numerical scheme to evolve the level set of DISF. It is well known that for numerical stability considerations, the step of the conventional numerical scheme to integrate H-J equation should satisfy the so-called CFL condition, which implies that in every time step the level set can move not more than one grid length. This severe restriction may considerably slow down the speed of convergence. We also note that some new techniques, by Hintermüller and Ring (2003) have also been developed recently which allow to dispense with the CFL condition numerically and thus make the level set based algorithm run much faster. Performing topology optimization in DISF framework with the use of those kinds of technique is also a very interesting research topic. Moreover, since narrow band and re-initialization scheme are often used for the solution of H-J equation to save computational effort and to enhance numerical stability, this may reduce the possibility of creating holes in the design domain.

Another one is related to the boundary evolution nature of the level set based-approach. It has been demonstrated by numerical experiments that in traditional DISF based approaches topology changes can only be achieved by pinching or merging of the boundaries, unlike traditional element-based approaches, it is very difficult to create new holes in the solid regions or to grow solid in void regions. As a result, as shown in Belytschko, Xiao and Parimi (2003), the convergence (to the optimal topology) will also be very slow even though, instead of resorting to the solution of H-J equation, optimality criteria method is employed to find the optimal nodal values of the implicit surface function. This can be attributed to the fact that topological derivative is not taken into consideration during the course of optimization. This will be discussed in more details in Section 4.

In order to overcome the above mentioned difficulties associated with the DISF based methods, in the present paper, a new approach for structural topology optimization based on dynamic implicit surface function is proposed. The ultimate goal of our research is to enhance the computational efficiency of the

DISF based approach for topology optimization of continuum structures. Implicit function is also used to describe the shape/topology of the structure, which is approximated in terms of its nodal values. Then, a relationship is established between the element stiffness and the values of the implicit surface function on its four nodes. In this way and with some non-local treatments of the design sensitivities, not only the shape derivative but also the topological derivative of the optimal design can be incorporated into the numerical algorithm in a unified way. Numerical experiments demonstrate that by employing this approach the computational efforts associated with DISF based algorithms can be saved. Clear optimal topologies free from any sign of numerical instability and smooth structural boundaries can be obtained simultaneously and efficiently.

The outline of this paper is as follows. In Section 2, the formulation of the optimization problem is given. In Section 3 we discuss the discrete form of the optimization problem. In Section 4, shape and topological derivatives and how to incorporate them into the same computational framework are discussed. Several examples are studied in Section 5. Finally some concluding remarks will be presented.

2. The optimization problem

In the following, we present the formulation of the optimization problem. The objective of our optimization problem is to minimize the compliance of a linearly elastic structure while satisfying the total volume constraint. Small deformation assumption is adopted here. Without loss of generality, discussions will be carried out only for 2D case. Extension to 3D case is quite straightforward. We assume that D is a reference design domain (ground structure, see Fig. 1 for reference), which includes all of the possible configurations of the structure during the course of optimization. Referring to the reference domain D and neglecting the volume force, we can define the optimal shape/topology design problem as a minimization of the work done by the external traction force as follows:

$$
\begin{aligned}
&P_\chi : \qquad (1)\\
&\text{Find } \chi(\mathbf{x}) \in L^\infty(D)\\
&\underset{\chi(\mathbf{x})}{\text{minimize}}\, l_\chi(\mathbf{u}) = \int_{S_t} \mathbf{p} \bullet \mathbf{u} dS\\
&\text{subject to:}\\
&a_\chi(\mathbf{u},\mathbf{v}) = \iint_D \chi(\mathbf{x}) C_{ijkl} u_{i,j} v_{k,l} d\Omega = \int_{S_t} p_i v_i dS \quad \text{for all } \mathbf{v} \in \mathbf{U}_{ad}\\
&G_\chi = \left(\iint_D \chi(\mathbf{x}) dV - \overline{V}\right) \le 0\\
&\chi(\mathbf{x}) = \begin{cases} 1 & \mathbf{x} \in \Omega \\ 0 & \mathbf{x} \in D \backslash \Omega \end{cases} .
\end{aligned}
$$

Here, $\mathbf{u} \in \mathbf{U}$ and $\mathbf{v} \in \mathbf{U}_{ad}$ are the displacement and test functions, respectively; $\chi(\mathbf{x})$ is the shape/topology characteristic function of the current configuration Ω occupied by the structure; C_{ijkl} denotes the components of the elasticity tensor. The sets of admissible displacement function and test function in bilinear form $a_\chi(\mathbf{u}, \mathbf{v})$are defined as $\mathbf{U} = \mathbf{U}_{ad} = \{\mathbf{w} \,|\mathbf{w} \in \mathbf{H}^1(\Omega)$ and $\mathbf{w} = \mathbf{0}$ on $S_\mathrm{u}\}$. S_u and $S_t (S_u \cup S_t = \partial\Omega,\ S_u \cap S_t = \phi)$ denote the displacement prescribed and traction prescribed boundaries of Ω, respectively; $\partial\Omega$ is the boundary of Ω, which is constituted by the points $\mathbf{x}$ such that $\phi(\mathbf{x}) = 0$; $\mathbf{p} \in \mathbf{H}^{1/2}(\partial\Omega)$ is the boundary traction; $\overline{V}$ is the prescribed total volume of the available material.

It is well-known that the above problem is ill-posed in the sense that generally no solution exists in the original design space (Cheng, Olhoff, 1981; Kohn, Strang, 1986; Allaire, Kohn, 1993). Either relaxation (Allaire, Kohn, 1993; Lurie, Cherkaev, 1982) or restriction (Ambrosio, Buttazzo, 1993; Haber, Bendsøe, Jog, 1996; Petersson, Sigmund, 1998) of the design space is required to make the problem well-posed. Moreover, we can also introduce some non-local effects into the problem formulation to guarantee the existence of solution (Borrvall, Petersson, 2001; Bourdin, 2001; Guo, Zhao, Gu, 2004b).

In DISF context, the problem is reformulated by introducing an implicit surface function ϕ, which replaces the characteristic function χ in P_χ and describes the shape/topology of the structure in the following way:

$$\begin{array}{lcll} \phi(x,t) & = & 0 & \text{on} \quad S = \partial\Omega \\ \phi(x,t) & > & 0 & \text{in} \quad \Omega \\ \phi(x,t) & < & 0 & \text{in} \quad D/\Omega\,. \end{array} \tag{2}$$

See Figs. 1 and 2 for reference.

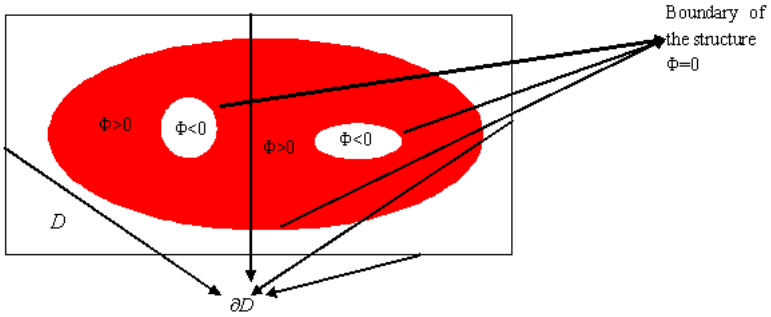

Figure 1. Design domain and the current configuration of the structure.

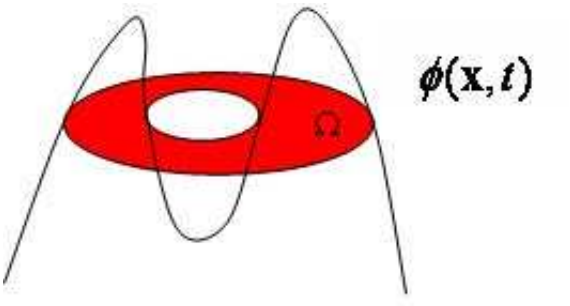

Figure 2. Shape topology representation by *DISF*

If we use ϕ as shape/topology design variable, the optimization problem can be reformulated as follows:

$$
\begin{aligned}
&P_\phi : \qquad (3)\\
&\text{Find } \phi(\mathbf{x}) \in L^\infty(D)\\
&\underset{\phi}{\text{minimize}}\, l_\phi(\mathbf{u}) = \int_{S_t} \mathbf{p} \bullet \mathbf{u} dS\\
&\text{subject to:}\\
&a_\phi(\mathbf{u},\mathbf{v}) = \iint_D H(\phi) C_{ijkl} u_{i,j} v_{k,l} dV = l_\phi(\mathbf{v}) = \int_{S_t} p_i v_i dS \quad \text{for all} \quad \mathbf{v} \in \mathbf{U}_{ad}\\
&G_\phi = (\iint_D H(\phi(\mathbf{x}))dV - \overline{V}) \leq 0\,.
\end{aligned}
$$

Here H is the Heaviside function.

It should be noted that the only difference between P_χ and P_ϕ is that the design variable has been changed from χ to ϕ. It is obvious that $\chi(\mathbf{x}) = H(\phi(\mathbf{x}))$. This formal change cannot alter the mathematical nature of the original optimization problem and therefore cannot regularize it.

3. Discrete formulation of the optimization problem

3.1. Discrete formulation of the optimization problem

Let us put the well-posedness of P_ϕ aside for a moment and still use it as the basis of numerical solution. In our approach, like in Belytschko, Xiao and Parimi (2003), the discrete problem is formulated in finite element framework. We will

approximate $\mathbf{u}$ and $\phi(\mathbf{x})$ by uniform 4-node quadrilateral element as:

$$\mathbf{u}^h(\mathbf{x}) = \sum_{I=1}^{NI} N_I(\mathbf{x})\mathbf{u}_I \tag{4}$$

$$\phi^h(\mathbf{x}) = \sum_{I=1}^{NI} N_I(\mathbf{x})\phi_I \,. \tag{5}$$

Here NI denotes the total number of nodes in FEM grid and $N_I(\mathbf{x})$ is the shape function of node I. The discrete form of P_ϕ now can be expressed as:

$$\begin{aligned}
&(P_\phi)^h : \\
&\text{Find } \phi^h(\mathbf{x}) \in L^\infty(D) \\
&\underset{\phi^h}{\text{minimize}}\, l_{\phi^h}(\mathbf{u}^h) = \int_{S_t} \mathbf{p}^h \bullet \mathbf{u}^h dS \\
&\text{subject to:} \\
&a_{\phi^h}(\mathbf{u}^h, \mathbf{v}^h) = \iint_D H(\phi^h(\mathbf{x}))C_{ijkl}u^h_{i,j}v^h_{k,l}dV = \int_{S_t} p^h_i v^h_i dS \\
&\qquad\qquad\qquad\qquad\qquad\qquad \text{for every} \quad \mathbf{v}^h \in \mathbf{U}^h_{ad} \\
&G_{\phi^h} = (\iint_D H(\phi^h(\mathbf{x}))dV - \overline{V}) \le 0 \,.
\end{aligned} \tag{6}$$

Here $\mathbf{U}^h_{ad}$ denotes the finite element space of the test functions in bilinear form. $\mathbf{p}^h = P_h\mathbf{p}$ with P_h denoting the projection operator from $\mathbf{H}^{1/2}(\partial\Omega)$ to the corresponding finite element space.

Using the discrete form of $a_{\phi^h}(\mathbf{u}, \mathbf{v})$, the element stiffness matrix can be obtained. In Belytschko, Xiao and Parimi (2003) this is done by direct numerical integration. In the present work, we will use a different approach. We take the elasticity tensor $C^{(e)}_{ijkl}$ as constant in each element and its value is related to the values of ϕ on its four nodes as:

$$C^{(e)}_{ijkl} = C_{ijkl}[\sum_{m=1}^{4}(H(\phi^{(e)}_m)/4)]^n \tag{7}$$

where $n \ge 1$ is a penalization parameter and $\phi^{(e)}_m$ is the value of ϕ on element e's m-th node.

The stiffness matrix of element e can be obtained as:

$$\mathbf{k}_{(e)} = [(\sum_{i=1}^{4} H(\phi^{(e)}_i)/4)]^n \iint_{V^e} \mathbf{B}^T\mathbf{D}^0\mathbf{B}dV^e = [(\sum_{i=1}^{4} H(\phi^{(e)}_i)/4)]^n \mathbf{k}^0_{(e)} \,. \tag{8}$$

Here $\mathbf{D}^0$ is the matrix form of the fourth-order elasticity tensor C_{ijkl}. $\mathbf{B}$ is the strain matrix and $\mathbf{k}^0_{(e)} = \iint_{V^e} \mathbf{B^T}\mathbf{D}^0\mathbf{B}dV^e$.

It will be shown later that a non-local effect can be introduced to the numerical solution process by this kind of stiffness smear-out scheme, which is crucial for obtaining the stable and regularized optimization results.

4. Shape and topological derivative and numerical solution aspects

4.1. Shape derivative of the objective functional

The optimal nodal values of ϕ_I will be solved by mathematical programming algorithm (MMA algorithm, Svanberg, 1987, in the present work). Compared with the approaches that employ numerical algorithms to evolve the level set of DIFS based on H-J equation, this kind of numerical treatment has the following advantages. Firstly, there is no severe restriction imposed by CFL condition, relatively large changes of the values of ϕ_I can be obtained in one iteration step and therefore fast convergence rate can be expected. Secondly, different kinds of constraints can be dealt with in a more straightforward way. Thirdly, topological derivative can be incorporated into the course of optimization in an easy way. This issue will be addressed in more details in the following.

In mathematical programming framework, sensitivity information is necessary for numerical solution. In the present approach, the sensitivities of the objective and constraint functional with respect to the design variables ϕ_I can be obtained as follows:

$$\begin{aligned}
&\partial l_{\phi^h}/\partial\phi_I = (\mathbf{F}_h)^{\mathbf{T}}(\partial\mathbf{u}^h/\partial\phi_I) = -(\mathbf{K}^{-1}\mathbf{F}_h)^{\mathbf{T}}(\partial\mathbf{K}/\partial\phi_I)\mathbf{u}^h \\
&= -(\mathbf{u}^h)^{\mathbf{T}}(\partial\mathbf{K}/\partial\phi_I)\mathbf{u}^h \\
&= -\frac{1}{4}\sum_{e=1}^{NBI} C_{ijkl}\, n[(\sum_{m=1}^{4} H(\phi_m^{(e)})/4)]^{n-1}[dH(\phi_I)/d\phi]((\mathbf{u}^h)^{(e)})^{\mathbf{T}}\mathbf{k}^0_{(\mathbf{e})}(\mathbf{u}^h)^{(e)}
\end{aligned} \tag{9}$$

$$\partial G_{\phi^h}/\partial\phi_I = \iint_D \delta(\phi^h(\mathbf{x}))N_I(\mathbf{x})dV\,. \tag{10}$$

Here *NBI* denotes the total number of elements which have the common node I, see Fig. 3 for reference. $\mathbf{K} = \sum_e \mathbf{k}_{(e)}$ is the global stiffness matrix. $\mathbf{F}^h$ is work equivalent nodal force vector, which is assumed to be design-independent. $(\mathbf{u}^h)^{(\mathrm{e})}$ denotes displacement vector of element e and δ represents the one dimensional Dirac function.

$H(\phi)$ in Eq. (9) are non-smooth functions, it should be regularized for numerical implementation purpose. As in Belytschko, Xiao and Parimi (2003), we take the regularized Heaviside function H_ϵ as:

$$H_\epsilon(x) = \begin{cases} \Delta_{\min} & x \le -\epsilon \\ \frac{1}{4}(1+\sin\frac{\pi x}{2\epsilon})^2 & -\epsilon < x < \epsilon \\ 1 & x \ge \epsilon \end{cases} \tag{11}$$

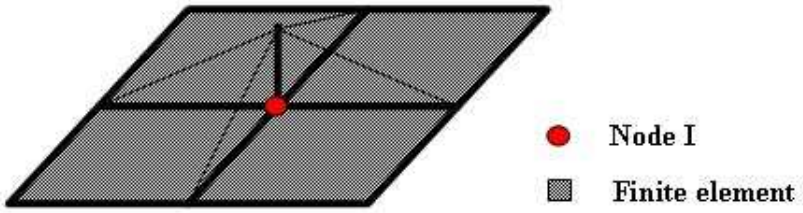

Figure 3. Node I and its neighbouring elements

where $\Delta_{\min}$ is a small parameter to ensuring the non-singularity of the global stiffness matrix. For numerical implementation, we take its value as 1.0e-03.

From Eq. (11) we have

$$\frac{dH_\varepsilon(x)}{dx} = \delta_\varepsilon(x) = \begin{cases} 0 & x \le -\varepsilon \\ \frac{\pi}{4\varepsilon}(1+\sin\frac{\pi x}{2\varepsilon})\cos(\frac{\pi x}{2\varepsilon}) & -\varepsilon < x < \varepsilon \\ 0 & x \ge \varepsilon\,. \end{cases} \tag{12}$$

Considering the characteristic of δ function, we know from Eq. (12) that $\partial l_{\phi^h}/\partial\phi_I$ is only non-zero when $\phi_I = 0$. This is also true for the value of A_I in Belytschko, Xiao and Parimi (2003, Eq. (35)). It means that only the (infinitesimal) changes of the values of ϕ on the boundary of the current configuration have the effect of improving the objective functional. The objective functional is blind to the infinitesimal change of the values of ϕ at the interior points of the domain (for $\mathbf{x} \notin \partial\Omega, |\phi(\mathbf{x})| > 0$). Therefore, we term this sensitivity shape sensitivity. If we use DISF as shape/topology design variable and calculate the sensitivity in the above-mentioned way, the topology of the structure can only be achieved by merging or pinching of the boundaries. As pointed out in Burger, Hackl and Ring (2004), it is usually very difficult or even impossible to create holes within existing shapes away from the boundaries or introduce new components at locations far from the boundaries. This is quite different from the traditional element-based approach, where the structural topology can be changed by deleting or adding elements in the whole area of the design domain. This also explains why the convergence of the DISF based approach is always slow compared with element-based approaches. If a regularized version of δ, such as $\delta_\epsilon(\phi)$ in Eq. (12) is used for numerical calculation, the support of $\partial l_{\phi^h}/\partial\phi_I$ and $\partial G_{\phi^h}/\partial\phi_I$ will be enlarged, the extent of the enlargement will be dependent on the value of ϵ. Thus, it can be concluded that the regularization of δ not only makes the calculation workable, but also introduces a boundary layer. Holes can be created or filled in this layer and solid material can also grow up from the boundary of this layer. Compared with the algorithms solely based on

level set evolution, this numerical trick makes the optimization algorithm "see" a little bit far from the boundary, but it still suffers from the disadvantage of low convergence rate because of the intrinsic local nature of the shape derivative. From the authors' point of view, to make the DISF based algorithms more computationally effective, global derivative should be incorporated into the course of optimization.

4.2. Mathematical justification of the present element formulation

Bourdin (2001) proposed a problem formulation for topology optimization of continuum structures aiming at minimizing the structural compliance. In this formulation the weak form of the equilibrium equation is written as:

$$\iint_D (F * \rho(\mathbf{x}))^n C_{ijkl} u_{i,j} v_{k,l} dV = \iint_D f_i v_i dV \tag{13}$$

where F is a convolution operator. It can be proved mathematically that this kind of treatment can regularize the original ill-posed problem formulation P_χ and guarantee the existence of the optimal solution. If instead of the material density ρ, one uses implicit surface function ϕ as the topology design variable and H_ε to regularize the Heaviside function H, then Eq. (13) can be rewritten as:

$$\iint_D (F * H_\epsilon(\phi(\mathbf{x}))^n C_{ijkl} u_{i,j} v_{k,l} dV = \iint_D f_i v_i dV \,. \tag{14}$$

From Eq. (14), it can be seen that Eq. (7) is somewhat the discrete counterpart of the stiffness interpolation of Bourdin's formulation in DISF framework. Therefore it is not surprising that the present element stiffness treatment can produce regularized and stable numerical results, which are free from numerical instabilities, such as check board pattern or mesh dependency. It is worth noting that the success of Bourdin's formulation can be attributed to the fact that the same non-local effect has been introduced to the problem formulation. Sigmund's filter approach (Sigmund, Petersson, 1998) has also successfully employed the non-local treatment to regularize the optimization problem numerically. In Belytschko, Xiao and Parimi (2003), the authors introduced a small number ϵ as the size of the support to obtain a regularized version of the Heaviside function. In fact, this treatment introduced a non-local effect into the numerical solution implicitly, thus stabilized the optimization process. Thus, ϵ can be seen as the filter radius in Sigmund's approach or the size of the support of the convolution operator F in Bourdin's approach. This may explain why stable numerical results can also be obtained even though they start from an ill-posed continuum formulation P_ϕ. Hence, the introduction of H_ε is not only due to numerical implementation purpose, but it also plays the role of ensuring the existence of the minimizer of the optimization problem.

4.3. Topological derivative of the objective functional

As pointed out by Reuiter and Keulen (2003), in DISF based optimization framework, shape derivative cannot measure the effects resulting from the creation of holes at the interior point of Ω. This is due to the fact that shape sensitivity obtained by taking the derivative with respect to ϕ_I can only provide local information resulting in very small (infinitesimal, theoretically) variations of the design variables. For ϕ_I's that are strictly greater than zero, very small variation of ϕ_I cannot change the value of $H(\phi_I)$. Thus, just as pointed out in Section 4.1, this information is not sufficient for topology optimization, since the topology change at the interior point of Ω can only be achieved by finite change of ϕ_I. See Fig. 4 for reference.

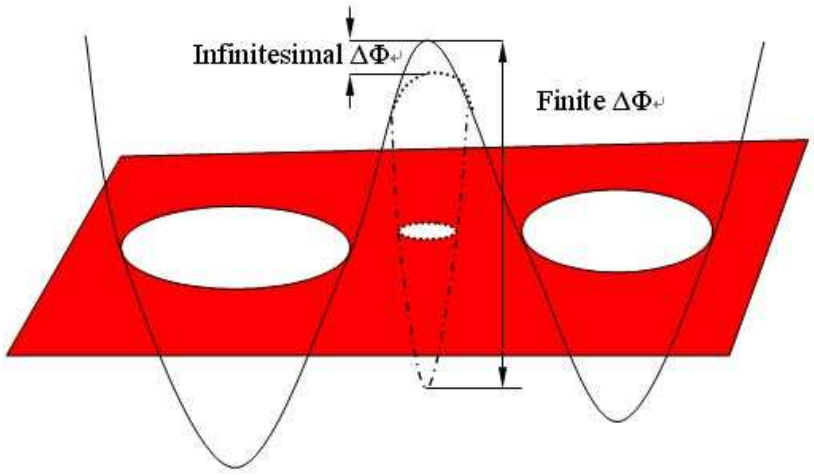

Figure 4. Topology change at the interior of Ω can only be achieved by finite change of ϕ

Topological derivative (Eschenauer, Kobelev, Schumacher, 1994; Sokolowski, Zochowski, 1999; Lewinski, Sokolowski, 2003; Cea et al., 2000; Garreau, Guillaume, Masmoudi, 2001) is another sensitivity measure that has been used recently by many researchers to solve topology optimization problems. Compared with the afore-mentioned shape derivative, it can account for the sensitivity of creating a hole at the interior point of design domain. In the language of DISF, it can account for the finite changes of the values of the implicit surface function at the interior points of the design domain.

The concept of topological derivative was first proposed in the engineering literature by Eschenauer, Kobelev and Schumacher (1994). It was established

based on the engineering intuition and derived with the application of Saint-Venant's principle. In their work, for finding the optimal shape and topology of elastic structures, they used topological derivative as a measure to determine where to insert a hole in the structure. The rigorous and more general mathematical framework of topological derivative was first established by Sokolowski and Zochowski (1999). In this framework, the topological derivative at an interior point $\mathbf{x}$ of the design domain is defined as:

$$TD(\mathbf{x}) = \lim_{|\omega|\to 0} \frac{J(S\backslash\omega) - J(S)}{|\omega|} \tag{15}$$

where S denotes the design domain, ω represents a small hole (ball for 3D case), centered at $\mathbf{x}$, that will be created. J is a structural response of interest. $|\omega|$ is the measure of ω. In this context, if J is taken as the total potential energy of the structure, with the help of asymptotic analysis, for 2D case and isotropic material, the corresponding topological derivative can be obtained as (also see Lewinski, Sokolowski, 2003, for reference):

$$TD(\mathbf{x}) = -\frac{1}{2\widetilde{E}}[(\overset{o}{\sigma}_I + \overset{o}{\sigma}_{II})^2 + 2(\overset{o}{\sigma}_I - \overset{o}{\sigma}_{II})^2] \tag{16}$$

here the quantities $\overset{o}{\sigma}_I$ and $\overset{o}{\sigma}_{II}$ are two principal stresses for the stress field of the original unperturbed structure. $\widetilde{E} = 4k\mu/(k+\mu)$ and k, μ denote the bulk and shear moduli of the isotropic material, respectively.

From the above results, it is clear that the topological derivative at a point $\mathbf{x}$ in the design domain is in some sense proportional to the strain energy density at this point. For traditional element based algorithms, if the density ρ^e of each element is used as the topology design variable, the sensitivity of the objective functional with respect to ρ^e is

$$\partial l/\partial\rho^e = -n(\rho^e)^{n-1}(\mathbf{u}^e)^T\mathbf{K}_0^e(\mathbf{u}^e) = -n(\rho^e)^{n-1}W_0^e \tag{17}$$

which is proportional to the strain energy density of the corresponding element. Thus, it can be concluded that in traditional element-based framework, the concept of topological derivative has already been employed, although somewhat implicitly. Therefore, it explains why the traditional element-based algorithm can find the outline of the optimal topology efficiently. In traditional element-based framework, holes can be created in the solid regions and solid material can grow up from the void areas of the design domain. In this aspect, the traditional element based approach has its advantage over the current version of the DISF based algorithm from the computational efficiency point of view.

At this point, a question arises naturally: can we make the DISF based algorithms work more efficiently without losing their advantage in description of geometry? It seems that a promising way to achieve this goal is to combine shape derivative with topological derivative in the same DISF based optimization framework. Burger's work is the first step along this line. In Burger, Hackl

and Ring (2004), topological derivative is introduced to accelerate the evolution of the zero level set by adding a source term to the level set equation. Numerical results show that the new approach based on shape and topological derivatives can successfully circumvent the obstacles in situations where the standard level set approach fails. In the present paper, another technique will be used to incorporate the topological derivative into the DISF based optimization framework.

As in Belytschko, Xiao and Parimi (2003), the value of ϕ is restricted to the interval of $[-\alpha, +\alpha]$, where α is a positive value and the width of regularization of $\delta(\phi)$ is set to be less than α, i.e. $\epsilon \leq \alpha$. In our approach, in order to take the topological derivative into consideration, we set $\epsilon > \alpha$. From Eqs. (11) and (12), it is clear that with the use of this approach, unlike the traditional DISF based method, all values of ϕ_I (not only the ϕ_I such that $|\phi_I| \leq \epsilon$) may have a contribution to the sensitivity of the objective functional. According to Eq. (9), it can be found that the contribution of the variation of these ϕ_I is also proportional to the element strain energy density, which is in some sense consistent with the topological derivative shown in Eq. (16). In this way, besides shape derivative, we incorporate the topological derivative into the DISF based optimization approach as well in a consistent manner. Numerical results demonstrate that this treatment considerably enhances the computational efficiency. It should be noted that to guarantee the accuracy of displacement calculation, the value of the regularized parameter ϵ in Eq. (12) should be less than α. But numerical experience shows that if we also take the value of ϵ in Eq. (12) to be greater than α, more smooth optimization results can be obtained with faster convergence rate. This may be attributed to the fact that this treatment has the effect of making a balance between the contributions of shape and topological derivatives in a non-linear way, which can help to accelerate the convergence process.

4.4. Numerical solution aspects

Based on the above formulation, we solve the shape/topology optimization numerically in the following way:

(1) Give the initial design domain D and set boundary and load conditions;
(2) Use uniform 4-node quadrilateral element to approximate the displacement field $\mathbf{u}$ and implicit surface function ϕ;
(3) Construct the initial implicit surface function $\phi = \phi_0$ by finite element approximation based on given node values and set $|\phi_0| \leq \alpha$;
(4) For each element, use Eqs. (7) and (8) to form its stiffness matrix based on the current value of ϕ ;
(5) Calculate the displacement field;
(6) Perform sensitivity analysis by Eqs. (9) and (10) with the use of regularized Dirac function and set $\varepsilon \geq \alpha$ (this implementation includes the topological derivative information in the process of optimization implicitly as discussed in the previous section);

(7) Call MMA optimization subroutine to calculate the new values of ϕ;
(8) Check the convergence criteria. If it has been satisfied then go to step (9); otherwise go to (4);
(9) Extract the zero level set of the implicit surface function and obtain the final shape and topology of the structure.

From numerical experiments, we found that for the test examples, this algorithm can find the right optimal topology of the structure in 30-40 iteration steps. The following steps are made just to change the local details of the structure. To accelerate the convergence rate and obtain more smooth boundaries, we can stop the MMA optimization process and switch seamlessly to the H-J equation based level set optimization algorithms described in Allaire, Jouve and Toader (2004), Wang, Wang and Guo (2004), since these algorithms are local in nature and are very powerful for local shape improvements.

5. Numerical examples

In this section, several numerical examples will be shown to demonstrate the effectiveness and efficiency of the present approach for the solution of topology optimization problems. The material data and dimensions for the problem are chosen non-dimensional since only qualitative results are considered. If not mentioned, the material parameters are: Young's modulus $E = 1.0$, Poisson's ratio $v = 0.3$. Plane stress status is assumed and the loading is $P = 1.0$. The bound α for ϕ is $\min(\Delta x, \Delta y)$ and ϵ is taken as $3 * \min(\Delta x, \Delta y)$ for both of the regularized Heaviside and Dirac functions. Here Δx and Δy are grid sizes along x and y directions, respectively.

5.1. Cantilever beam loaded on the right side

The problem under investigation is defined in Fig. 5. The displacement is set to zero along the left side of the design domain. A vertical load is imposed on the middle point of the right side. The dimensions of the initial design domain are: length $L = 8.0$, width $W = 5.0$ and thickness $t = 1.0$. The available volume of the material is set to $\overline{V} = 16$. The design domain is discretized by 80×50 finite elements. Figs. 6-7 show the optimization processes for different initial designs. In this and the following examples, we first carry out the optimization with the use of the proposed approach. Once clear topologies are obtained, then we switch to the level-set based algorithm proposed in Allaire, Jouve and Toader (2004), Wang, Wang and Guo (2004) for further local boundary shape improvements. In this way, simultaneous topology and shape optimization is achieved in a unified way. It can be seen from these figures that although the final result is identical to that obtained in Belytschko, Xiao and Parimi (2003), the histories of the topology evolution are quite different from each other. In Belytschko, Xiao and Parimi (2003), holes can only be created near the boundaries and the change of topology is mainly achieved by boundary motion.

Figure 5. Design domain of Example 5.1

For the present approach, the topology change can occur globally. Materials can grow up from the regions far from the boundaries and the small "islands" without mechanical relevance can be eliminated from the design domain very quickly, since no CFL condition is imposed on the algorithm. Compared with the previous DISF-based approach, the convergence of the present approach is faster. Clear structural topology can be obtained within 30 steps even though the initial design looks like complex. The obtained optimization results are quite smooth and free from any sign of numerical instability.

5.2. Cantilever beam loaded at the right bottom

The same initial design domain is used in this example. In this case, the external force is applied on the right bottom corner. The volume constraint is set to $\overline{V} = 12$. The design domain is also discretized by 80×50 finite elements.

Figs. 8-9 show the optimization processes for different initial designs. It can be seen that the convergence processes are very fast for both cases. After about 20-30 iterations, the optimal topology identical to that presented in the literature can be produced. Once the outline of the structural topology is obtained, we can switch to the H-J equation based level set optimization approach to improve the local boundary shape of the structure.

6. Concluding remarks

In this paper a new approach for structural topology optimization based on dynamic implicit surface function(DISF) is proposed. DISF is used to describe the

shape/topology of the structure, which is approximated in terms of its nodal values. Then a relationship is established between the element stiffness and the values of the implicit surface function on its four nodes. In this way and with some non-local treatments of the design sensitivities, not only the shape derivative but also the topological derivative of the optimal design can be incorporated in the numerical algorithm in a unified way. The reasons for the success of the previous proposed DISF based optimization for the elimination of numerical instabilities have also been clarified. Numerical examples demonstrate that combining shape design sensitivity and topological derivative within the same DISF based optimization framework can help to find the optimal topology in an efficient way. It seems that the present approach can share both the advantages of the element-based and DISF-based optimization approaches.

Acknowledgements

The financial support for this research was provided by *China Natural Science Foundation* under the grants No. 10102003, No. 10472022, No. 10225212, No. 10332010, No. 50128503, and No. 50390063, and by the Research Grants Council of Hong Kong SAR (Project No. CUHK4164/03E). These supports are gratefully acknowledged. The first author also thanks Prof. Svanberg for providing the MMA optimization subroutine. The authors also thank the anonymous referees for their helpful comments.

References

Allaire, G., Jouve, F. and Toader, A.M. (2002) A level set method for shape optimization. *Comptes Rendus de l'Académie des Sciences, Serie I* **334**, 1125-1130.

Allaire, G., Jouve, F. and Toader, A.M. (2004) Structural optimization using sensitivity analysis and a level-set method. *Journal of Computational Physics* **194**, 363-393.

Allaire, G. and Kohn, R.V. (1993) Optimal design for minimum weight and compliance in plane stress using extremal microstructures. *European Journal of Mechanics/A* **12**, 839-878.

Ambrosio, L. and Buttazzo, G. (1993) An optimal design problem with perimeter penalization. *Calculus of Variations* **1** 55-69.

Belytschko, T., Xiao, S.P. and Parimi, C. (2003) Topology optimization with implicit functions and regularization. *International Journal for Numerical Methods in Engineering* **57**, 1177-1196.

Bendsøe, M.P. (1989) Optimal shape design as a material distribution problem. *Structural Optimization* **1**, 193-202.

Bendsøe, M.P. (1999) Variable-topology optimization: status and challenges. In: W. Wunderlich, ed., *Proceedings of European Conference on Computational Mechanics*, München, Germany, August 31-September 3. Universität München, Paper No.137.

Bendsøe, M.P. and Kikuchi, N. (1988) Generating optimal topologies in optimal design using a homogenization method. *Computer Methods in Applied Mechanics and Engineering*, **71**, 197-224.

Borrvall, T. and Petersson, J. (2001) Topology optimization using regularized intermediate density control. *Computer Methods in Applied Mechanics and Engineering* **190**, 4911-4928.

Bourdin, B. (2001) Filters in topology optimization *International Journal of Numerical Methods in Engineering* **50**, 2143-2158.

Burger, M., Hackl, B. and Ring, W. (2004) Incorporating topological derivatives into level set methods. *Journal of Computational Physics* **194**, 344-362.

Cea, J.S., Garreau, S., Guillaume, P. and Masmoudi, M. (2000) The shape and topological optimizations connection. *Computer Methods in Applied Mechanics and Engineering* **188**, 713-726.

Cheng, G.D. and Guo, X. (1997) *Epsilon*-relaxed approach in structural topology optimization. *Structural Optimization* **13**, 258-266.

Cheng, G.D. and Olhoff, N. (1981) An investigation concerning optimal design of solid elastic plates. *International Journal of Solids and Structures* **16**, 305-323.

Duysinx, P. and Bendsøe, M.P. (1998) Topology optimization of continuum structures with local stress constraints. *International Journal for Numerical Methods in Engineering* **43**, 1453-1478.

Eschenauer, H.A., Kobelev, V.V. and Schumacher, A. (1994) Bubble method for topology and shape optimization of structures. *Structural Optimization* **8**, 42-51.

Eschenauer, H.A. and Olhoff, N. (2001) Topology optimization of continuum structures: A review. *Applied Mechanics Review* **54**, 331-390.

Garreau, S., Guillaume, P. and Masmoudi, M. (2001) The topological asymptotic for PDE systems: The elasticity case. *SIAM Journal on Control and Optimization* **39**, 1756-1778.

Guo, X., Zhao, K. and Gu, Y.X. (2004a) Topology optimization with design-dependent loads by level set approach. Submitted to *S*tructural and Multidisciplinary Optimization.

Guo, X., Zhao, K. and Gu, Y.X. (2004b) A new density-stiffness interpolation scheme for topology optimization of continuum structures. *Engineering Computations* **21**, 9-22.

Haber, R.B., Bendsøe, M.P. and Jog, C.S. (1996) A new approach to variable-topology shape design using a constraint on the perimeter. *Structural Optimization* **11**, 1-12.

Hintermüller, M. and Ring, W. (2003) A second order shape optimization approach for image segmentation. *SIAM Journal on Applied Mathematics* **64**, 442-467.

Kohn, R.V. and Strang, G. (1986) Optimal design and relaxation of variational problems. *Communications on Pure and Applied Mathematics*, **39**, 1-25 (PART I), 139-182 (PART II) and 353-377 (PART III).

Lewinski, T. and Sokolowski, J. (2003) Energy change due to the appearance of cavities in elastic solids. *International Journal of Solids and Structures*, **40**, 1765-1803.

Lurie, K.A. and Cherkaev, A.V. (1982) Regularization of optimal design problems for bars and plates. *Journal of Optimization Theory and Applications* **37**, 499-522 (PART I), 523-543 (PART II) and **42**, 247-282 (PART III).

Osher, S.J., Fedkiw, R.P. (2003) *Level set and dynamic implicit surfaces.* Springer.

Osher, S.J. and Santosa, F. (2001) Level set methods for optimization problems involving geometry and constraints I. Frequence of a two density inhomogeneous drum. *Journal of Computational Physics* **171**, 272-288.

Petersen, N.L. (2000) Maximization of Eigenvalues using topology optimization. *Structural and Multidisciplinary Optimization* **20**, 2-12.

Petersson, J. and Sigmund, O. (1998) Slope constrained topology optimization. *International Journal for Numerical Methods in Engineering* **41**, 1417-1434.

Rozvany, G.I.N., Zhou, M. and Birker, T. (1992) Generalized shape optimization without homogenization. *Structural Optimization* **4**, 250-252.

de Ruiter, M.J. and van Keulen, F. (2003) The topological derivative in the topology description function approach. *Preprint.*

de Ruiter, M.J. and van Keulen, F. (2004) Topology optimization using a topology description function. *Structural and Multidisciplinary Optimization* **26**, 406-416.

Sethian, J.A. and Wiegmann, A. (2000) Structural boundary design via level set and immersed interface methods. *Journal of Computational Physics* **163**, 489-528.

Sigmund, O. and Petersson, J. (1998) Numerical instabilities in topology optimization. *Structural and Multidisciplinary Optimization* **16**, 68-75.

Sokolowski, J. and Zochowski, A. (1999) On the topological derivative in shape optimization. *SIAM Journal on Control and Optimization* **37**, 1251-1272.

Svanberg, K. (1987) The method of moving asymptotes-a new method for structural optimization. *International Journal of Numerical Methods in Engineering* **24**, 359-373.

Wang M.Y. and Wang, X.M. (2004) "Color" level sets: A multi-phase method for structural topology optimization with multiple materials. *Computer Methods in Applied Mechanics and Engineering* **193**, 469-496.

WANG, M.Y., WANG, X.M.and GUO, D.M. (2003) A level set method for structural topology optimization. *Computer Methods in Applied Mechanics and Engineering* **192**, 227-246.

WANG, X.M., WANG, M.Y. and GUO, D.M. (2004) Structural shape and topology optimization in a level-set framework of region representation. *Structural and Multidisciplinary Optimization* **27**, 1-19.

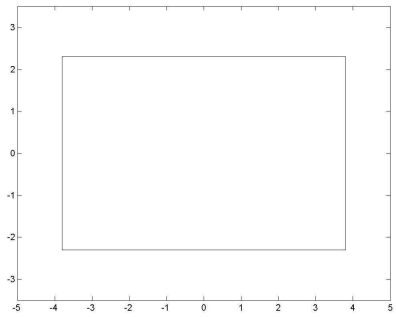

(a) Step 1

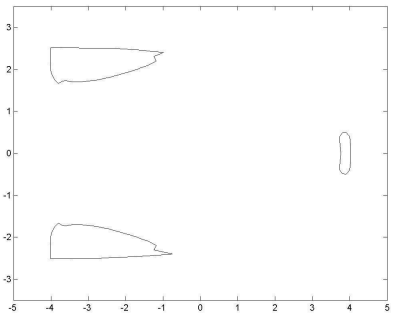

(b) Step 3

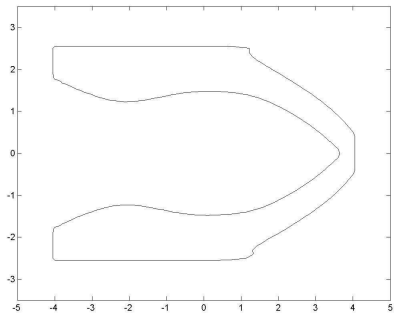

(c) Step 8

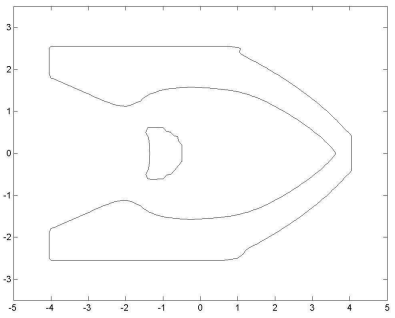

(d) Step 12

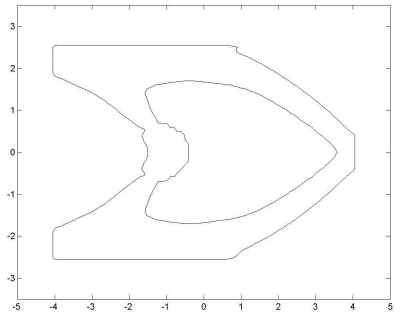

(e) Step 15

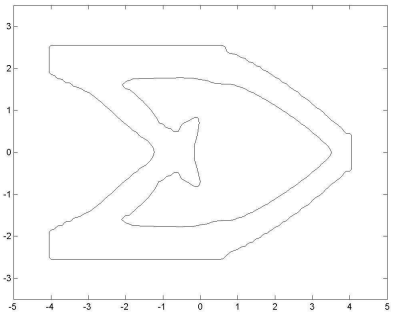

(f) Step 17

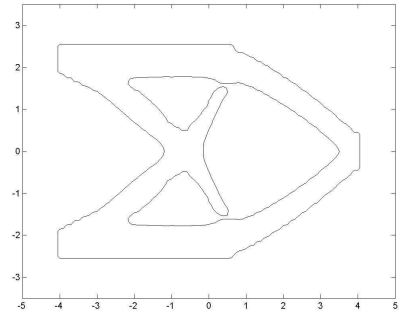

(g) Step 18

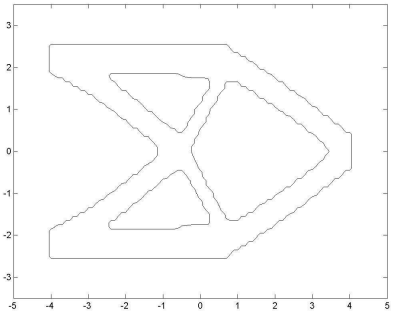

(h) Step 30

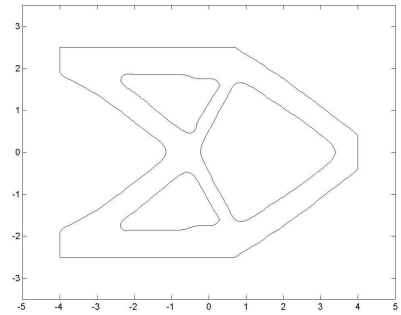

(i) Step 31

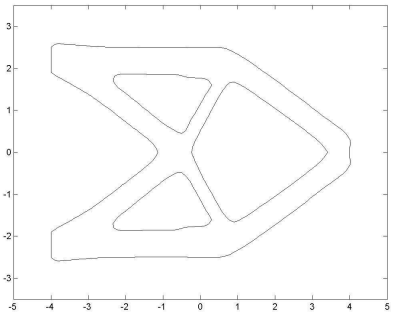

(j) Step 50

(k) DISF at step 30

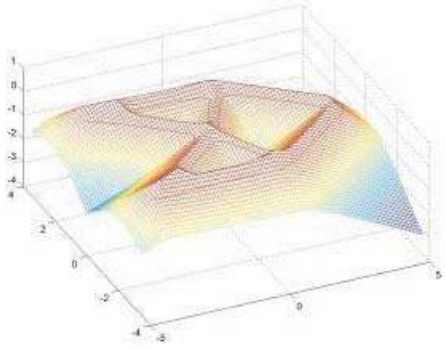

(l) DISF at step 50

Figure 6. Optimization process for example 5.1 from solid initial design

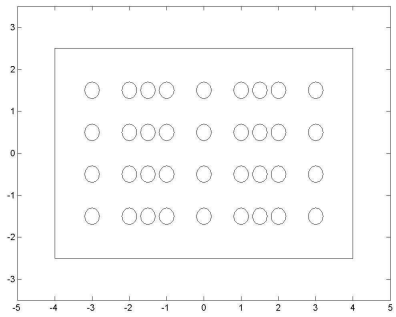

(a) Step 1

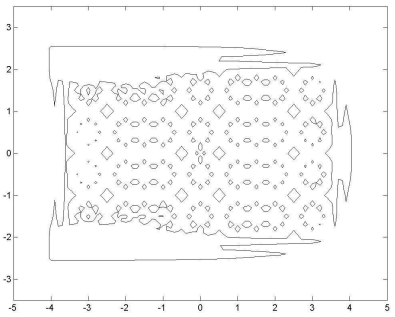

(b) Step 5

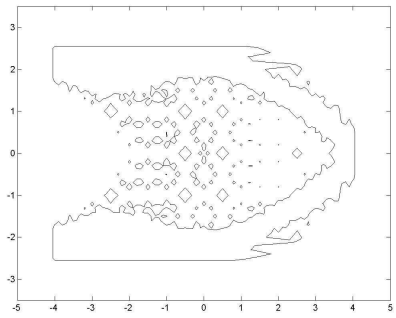

(c) Step 10

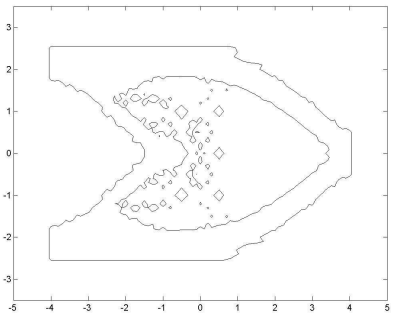

(d) Step 15

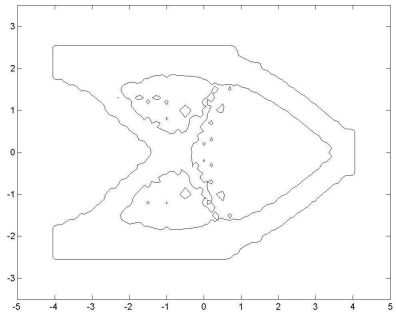

(e) Step 18

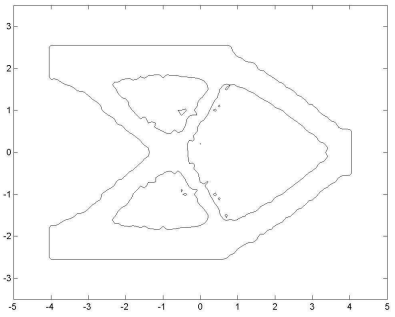

(f) Step 20

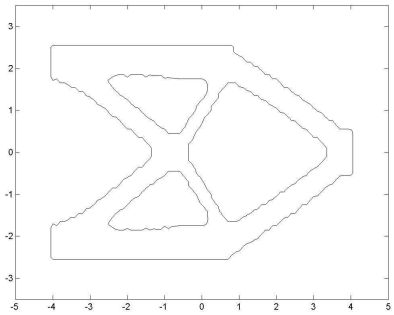

(g) Step 25

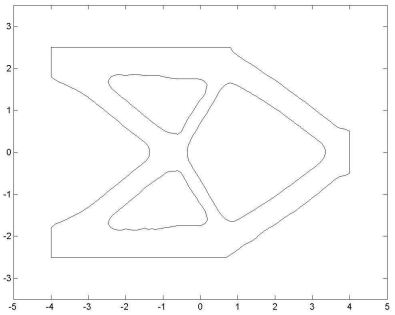

(h) Step 26

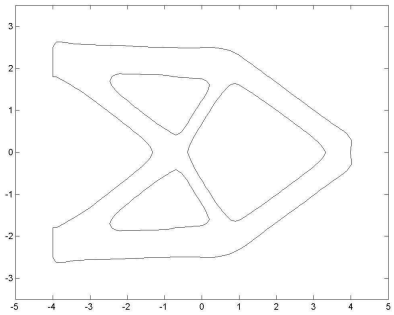

(i) Step 45

Figure 7. Optimization process of example 5.1 from initial design with many small holes

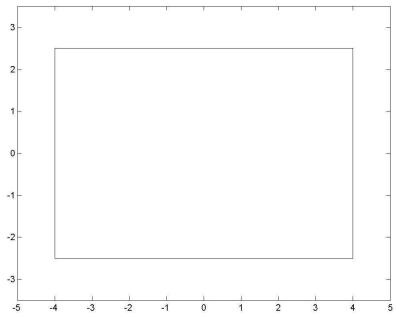

(a) Step 1

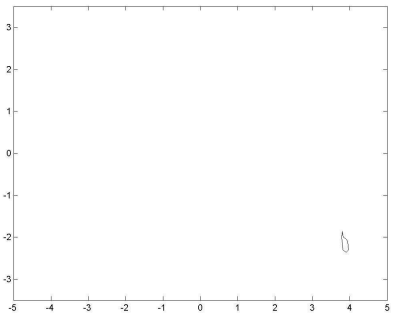

(b) Step 2

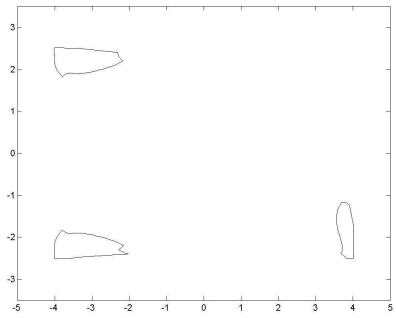

(c) Step 4

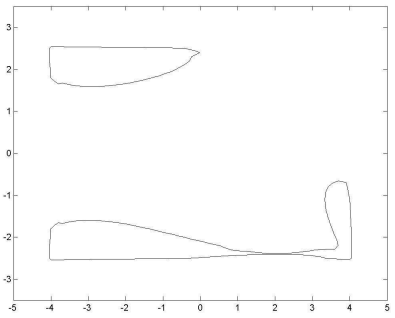

(d) Step 5

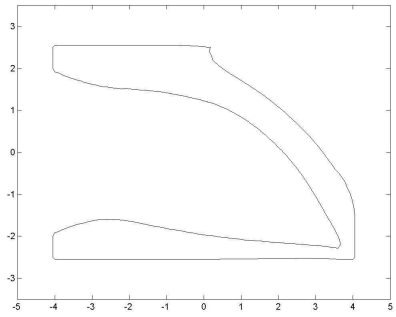

(e) Step 9

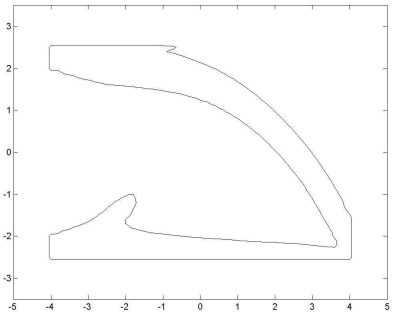

(f) Step 14

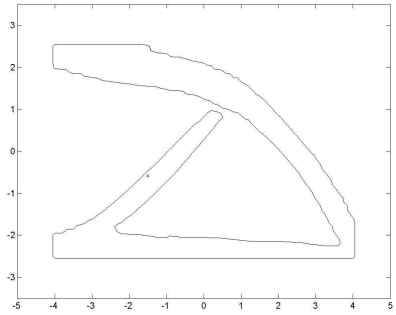

(g) Step 19

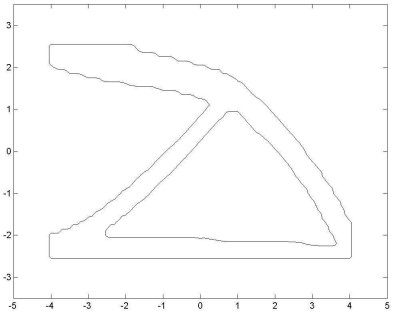

(h) Step 30

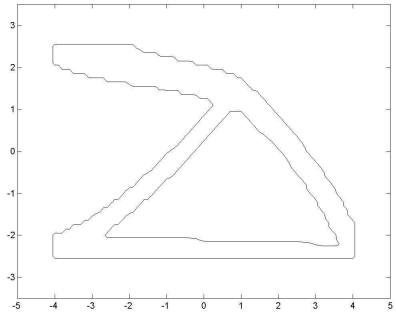

(i) Step 31

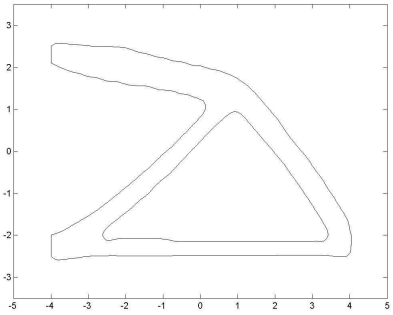

(j) Step 55

(k) DISF at step 30

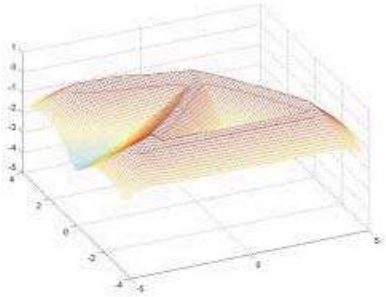

(l) DISF at step 55

Figure 8. Optimization process for example 5.2 from solid initial design

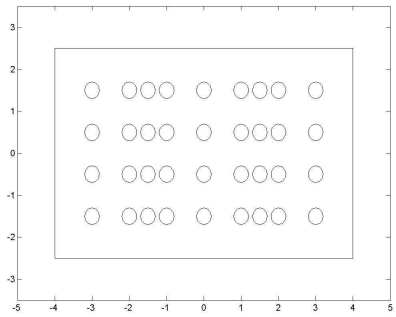

(a) Step 1

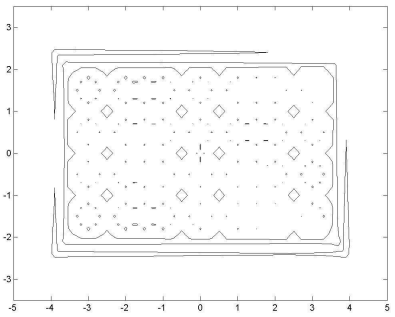

(b) Step 3

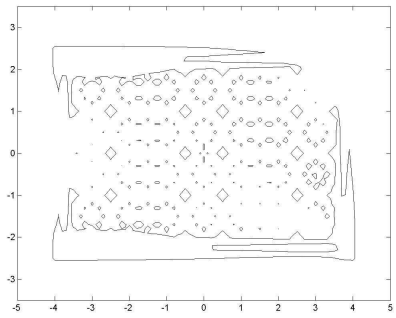

(c) Step 5

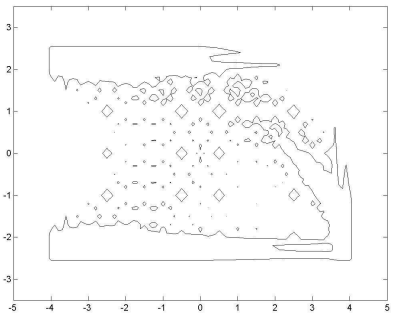

(d) Step 8

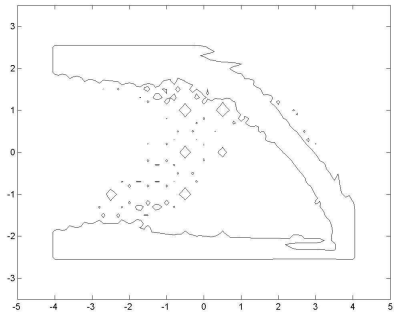

(e) Step 12

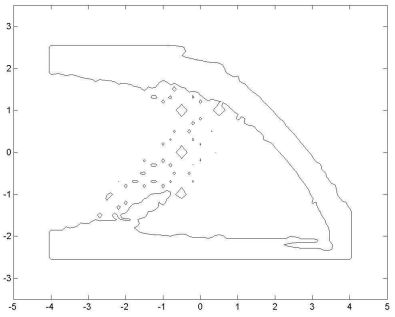

(f) Step 15

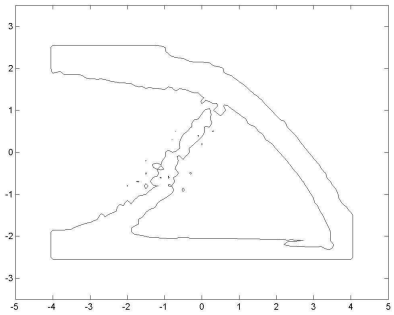

(g) Step 18

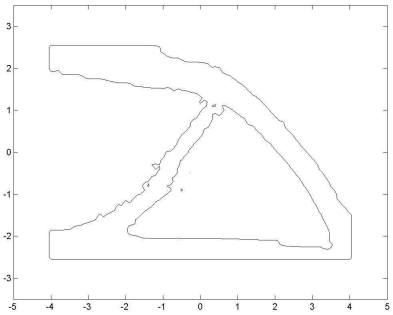

(h) Step 20

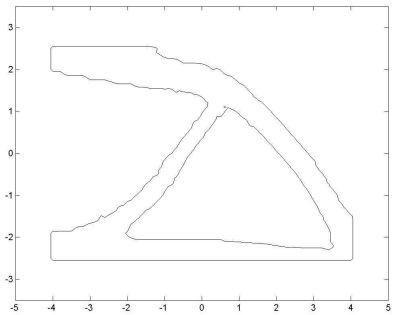

(i) Step 22

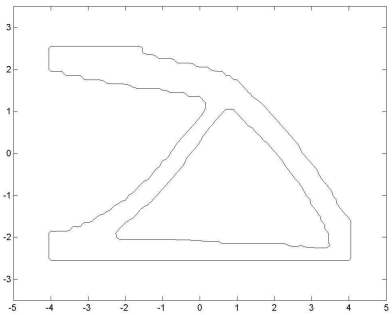

(j) Step 35

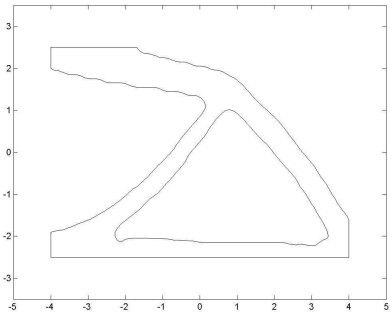

(k) Step 36

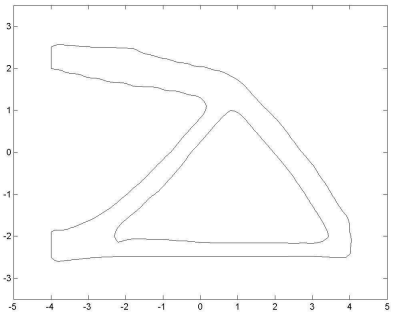

(l) Step 45

Figure 9. Optimization process of example 5.2 from initial design with many small holes